Article

Comparison of Electrical Properties of Viruses Studied by AC Capacitance Scanning Probe Microscopy

Robert I. MacCuspie, Nurxat Nuraje, Sang-Yup Lee, Anne Runge, and Hiroshi Matsui

J. Am. Chem. Soc., **2008**, 130 (3), 887-891 • DOI: 10.1021/ja075244z

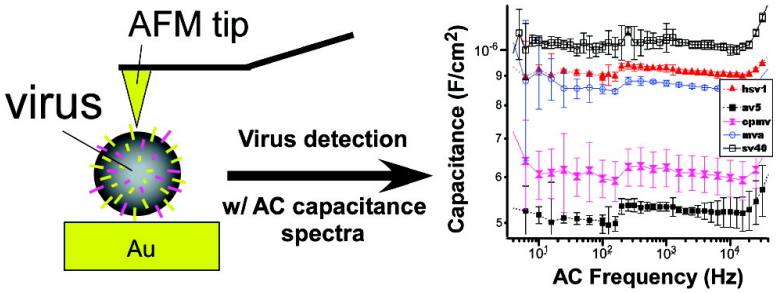

More About This Article

Additional resources and features associated with this article are available within the HTML version:

- Supporting Information
- Access to high resolution figures
- Links to articles and content related to this article
- Copyright permission to reproduce figures and/or text from this article

View the Full Text HTML

J|A|C|S
ARTICLES
Published on Web 12/20/2007

Comparison of Electrical Properties of Viruses Studied by AC Capacitance Scanning Probe Microscopy

Robert I. MacCuspie,† Nurxat Nuraje, Sang-Yup Lee,‡ Anne Runge, and Hiroshi Matsui*

Department of Chemistry, Hunter College, and The Graduate Center, The City University of New York, 695 Park Avenue, New York, New York 10021

Received July 13, 2007; E-mail: hmatsui@hunter.cuny.edu

Abstract: Capacitances of five types of viruses, adenovirus type 5 (AV5), herpes simplex virus type 1 (HSV1), simian virus 40 (SV40), vaccinia (MVA), and cowpea mosaic virus (CPMV), were compared by AC capacitance scanning probe microscopy. This technique, using a Pt-coated AFM tip as an electrode to probe capacitance of materials between the tip and a bottom electrode, has been applied to study surface structures of semiconductors and polymers with nanometer spatial resolution; however, biological samples at the nanoscale have not been explored by this technique yet. Because most biological cells are poor conductors, this approach to probe electric properties of cells by capacitance is logical. This scanning probe technique showed that each virus has distinguishable and characteristic capacitance. A series of control experiments were carried out using mutant viruses to validate the origin of the characteristic capacitance responses for different viruses. A mutation on the capsid in HSV1 with green fluorescence proteins increased capacitance from 9×10^{-6} to 1×10^{-5} F/cm^2 at the frequency of 10^4 Hz. Herpes simplex virus type 2 (HSV2) decreased capacitance when its envelope and glycoproteins were chemically extracted. These control experiments indicate that dielectric properties of capsid proteins and envelope glycoproteins significantly influence overall dielectric constants of viruses. Because those capsid proteins and glycoproteins are characteristic of the virus strain, this technique could be applied to detect and identify viruses at the single viron level using their distinct capacitance spectra as fingerprints without labeling.

Introduction

Electrical properties of biological cells have attracted broad interest from fundamental to applied sciences. For example, dielectric constants of cells could be influenced by locations and distributions of peptides, DNAs, and RNAs due to their individual dielectric response to AC frequency. These characteristic electronic properties of cells have been applied for their assay, separation, imaging, and quantification.[1−8] Recently, AC capacitance and impedance measurements have attracted interest for the applications in biomolecular systems since they do not require extra complex sample preparation procedures such as staining and manipulation of cells.[9] Because external AC fields can also trap a single cell by dielectrophoresis, the detection of cells with an extreme low detection limit could be achieved by monitoring impedance or capacitance changes before and after the cell binding event on electrodes.[10,11] Therefore, it is advantageous to apply AC capacitance measurements for biological cell detection since AC fields probe the polarization responses of low dielectric materials that possess relatively high resistance, and it is quite logical to probe electric properties of biological cells by capacitance since they are not highly conductive.

While the dielectric properties of cells have been investigated extensively, the dielectric properties of viruses have not been characterized yet even though pathogen identification is of continued importance in the area of medical diagnostics and biological warfare defense. The conventional detection of viruses at the nanoscale is more difficult compared to the detection of cells at the microscale in their low concentration due to their sizes. However, AC capacitance detection with atomic force microscope (AFM) could have an advantage for smaller virus detection. When a Pt-coated tip of AFM is applied as a

† Current address: Air Force Research Lab, Materials and Manufacturing Directorate, Wright-Patterson Air Force Base, OH 45433.

‡ Current address: Department of Chemical Engineering, Yonsei University, Seoul, 120-749, South Korea.

(1) Giaever, I.; Keese, C. R. *Nature* **1993**, *366*, 591−592.
(2) Asami, K.; Gheorghiu, E.; Yonezawa, T. *Biophys. J.* **1999**, *76*, 3345−3348.
(3) Horrocks, B. R.; Mirkin, M. V.; Pierce, D. T.; Bard, A. J.; Nagy, G.; Toth, K. *Anal. Chem.* **1993**, *65*, 1213−1224.
(4) Xiao, C.; Lachance, B.; Sunahara, G.; Luong, J. H. T. *Anal. Chem.* **2002**, *74*, 1333−1339.
(5) Tlili, C.; Reybier, K.; Geloen, A.; Ponsonnet, L.; Martelet, C.; Ben Ouada, H.; Lagarde, M.; Jaffrezic-Renault, N. *Anal. Chem.* **2003**, *75*, 3340−3344.
(6) Cherniavskaya, O.; Chen, L. W.; Weng, V.; Yuditsky, L.; Brus, L. E. *J. Phys. Chem. B* **2003**, *107*, 1525−1531.
(7) Hilton, A. M.; Lynch, B. P.; Simpson, G. J. *Anal. Chem.* **2005**, *77*, 8008−8012.
(8) Wilburn, J. P.; Wright, D. W.; Cliffel, D. E. *Analyst* **2006**, *131*, 311−316.
(9) Sohn, L. L.; Saleh, O. A.; Facer, G. R.; Beavis, A. J.; Allan, R. S.; Notterman, D. A. *Proc. Natl. Acad. Sci. U.S.A.* **2000**, *97*, 10687−10690.
(10) Beck, J. D.; Shang, L.; Marcus, M. S.; Hamers, R. J. *Nano Lett.* **2005**, *5*, 777−781.
(11) Bhatt, K. H.; Grego, S.; Velev, O. D. *Langmuir* **2005**, *21*, 6603−6612.

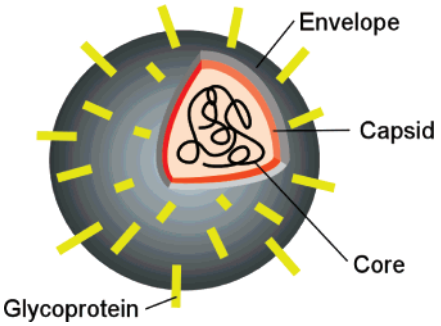

Figure 1. Representative illustration of the typical structure of viruses examined in this study. Two shells, envelopes and capsids, surround the core containing nucleic acids.

nanometer-sized electrode and a virus particle is located between the AFM tip and bottom electrodes, the impedance and the capacitance of viruses can be measured as AC fields are applied between electrodes. AC capacitance scanning probe microscopy (AC-SPM) was recently applied for characterization of various semiconductors and polymers with the spacial resolution in nanometers.[12−14] Recently, a nanoscale electrochemical probe was also demonstrated to probe electron transfers and ion flux mechanisms by penetrating cell membranes;[15] however, biological samples at the nanoscale have not been explored by this technique extensively. Many viruses have a structure consisting of an envelope as a shell, DNAs/RNAs in a core, and a capsid layer between the core and the envelope (Figure 1). Each virus has distinct capsid proteins and glycoproteins, which are distributed at specific positions throughout the capsid and the envelope. If the dielectric properties of those characteristic proteins affect the overall dielectric constants of viruses significantly, each virus may possess distinct capacitance. Under this hypothesis, we examined seven different viruses using AC-SPM. In this report, capacitances at higher AC frequency were compared for the virus identification to avoid complex ionic effects that could influence virus capacitance measurements due to the charge screening at electrode−fluid interfaces when capacitances are measured in solution.[9] The AC-SPM technique showed that each virus has distinct capacitance and modification of the envelope and the capsid of the same virus strain altered their capacitances. Since proteins in the envelope and the capsid were observed to have a significant contribution to the overall capacitances of viruses, this technique has the potential to be developed as virus detection and identification platforms through the analysis of their distinct capacitance spectra.

Experimental Section

Materials. Polystyrene (PS) nanoparticles (Polysciences, Warrington, PA) and poly(methyl methacrylate) (PMMA) nanoparticles (Bangs Labs, Fishers, IN) in the diameter of 100 nm were used as a standard for viral capacitance measurements. All purchased particles were diluted to 10^7 particles/mL, on the basis of the manufacturer's specifications of initial particle concentration in particles per milliliter. Serial dilutions to the final concentration of 10^7 particles/mL were performed; however, ultimately the precise concentration of particles in the final solution

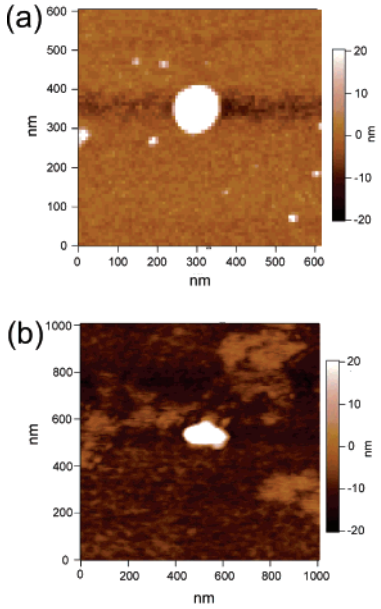

Figure 2. Representative AFM images of (a) HSV1 and (b) MVA. Most viruses examined in this report are spherical, as shown in (a), whereas MVA is the only virus whose shape is oval, as shown in (b).

was not known. In the preparation of viral samples, the precise concentration was not required to be known when one was interested in measuring capacitances of the discretely deposited particles on a substrate since there were broad ranges of concentration for which deposition of nanoparticles on surfaces created suitable samples for AFM analysis of single nanoparticle. Then, 10 μL of solution was dropped on gold substrates (Asylum Research, Santa Barbara, CA), working as another electrode. For each polymer nanoparticle in the figures, at least 50 particles locating different spots were chosen to measure their capacitances. During the study, different conductive tips were used on different days and different sample preps. The collected capacitance spectra were averaged and plotted against the AC frequency with error bars.

Adenovirus type 5 (AV5) was used as received from American Type Cell Culture (VR-1516). Titered stocks of simian virus 40 (SV40) and vaccinia (MVA) were obtained from Drs. Zhiping Ye and Michael Merchlinsky (all at FDA/CBER), respectively. Herpes simplex virus types 1 (HSV1) and 2 (HSV2), and HSV1 green fluorescence protein (GFP) mutants were graciously donated by Dr. Andrea Bertke (FDA/CBER). Cowpea mosaic virus (CPMV) was donated by Prof. John Johnson and used as received. Most viruses examined in this report were spherical, while MVA was the only virus whose shape was oval, and these viruses had the height of 20 ± 3 nm due to collapsing on the substrate based on their AFM images (Figure 2). The size of each virus was 75 ± 10 nm for AV5, 55 ± 3 nm for SV40, 270 ± 20 nm × 180 ± 30 nm for MVA, 170 ± 20 nm for HSV, and 25 ± 3 nm for CPMV. To create a series of spiked samples for analysis, 10-fold serial dilutions with distilled water were performed from virus stocks with known concentrations. The envelopes of the HSV2 virons were removed by a freon extraction. Freon was used as received from Fisher and added to a virus stock solution in a 1:1 volume/volume ratio. The mixture was vortexed for 30 s and then centrifuged at 14k rpm for 30 s. Then the aqueous layer containing the virus with no envelopes was collected.

Impedance/Capacitance Measurements of Polymer and Virus Particles. To develop a suitable interface between the AFM and the impedance analyzer that would not compromise extreme sensitivity requirements, a stand-alone MFP-3D AFM (Asylum Research, Santa Barbara, CA) was outfitted with custom modifications. Platinum-coated tips with a radius of curvature of less than 40 nm and spring constant near 40 N/m were used for topological AFM imaging and electrical measurements (Mikromasch NSC15-Ti/Pt, Wilsonville, OR; Nanosen-

(12) Layson, A.; Gadad, S.; Teeters, D. *Electrochim. Acta* **2003**, *48*, 2207−2213.
(13) Shao, R.; Kalinin, S. V.; Bonnell, D. A. *Appl. Phys. Lett.* **2003**, *82*, 1869−1871.
(14) Pingree, L. S. C.; Martin, E. F.; Shull, K. R.; Hersam, M. C. *IEEE Trans. Nanotechnol.* **2005**, *4*, 255−259.
(15) Fasching, R. J.; Bai, S. J.; Fabian, T.; Prinz, F. B. *Microelectron. Eng.* **2006**, *83*, 1638−1641.

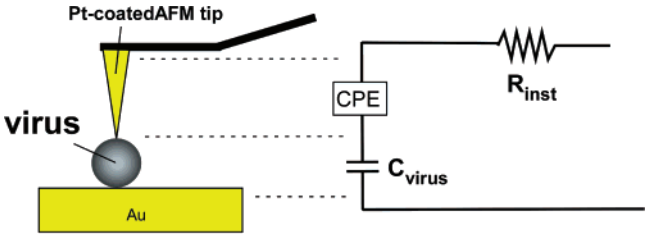

Figure 3. Probe configuration and its circuit model of the AC capacitance SPM. C_{virus} is capacitance of virus, CPE is a constant-phase element representing frequency-dependent capacitance and resistance of AFM tip and air,[5,13] and R_{inst} is resistance of the instrument.

sors PPP-NCHPt, NanoAndMoreUSA, Lady's Island, SC). Noncontact mode images were collected to find particles of interest while minimizing tip wear and extending lifetime of the Pt coating on the AFM tips. The tip end was positioned precisely at the center of the virus and nanoparticle using a computer-controlled closed-loop scanner. A constant force of 10−500 nN was applied throughout all capacitance measurements.

Humidity was controlled for all AC-SPM experiments by monitoring the humidity inside the acoustic isolation hood chamber. To control humidity levels between 10 and 90%, an ultrasonic humidifier was fitted with a connection to plumb a pipe into the acoustic AFM hood such that water vapor could flow into the acoustic hood chamber and increase the humidity. The samples were left in an acoustic isolation hood chamber at constant temperature and humidity overnight to reach equilibrium.

A Solartron 1260 frequency response analyzer with a Solartron 1296 dielectric interface (AMETEK, Paoli, PA) was used for the collection of impedance and capacitance spectra. The capacitance values were obtained after the data fitting of the measured impedance data whose circuit model is given in Figure 3. This circuit model was determined from control experiments of the model nanoparticles with the AC-SPM instrument. Briefly, the fitting to the equation in series with virus capacitance, cable inductance, and other frequency-dependent capacitance contributed from conductive AFM cantilever, air, leakage current, and loss parameter determined constants in the frequency-dependent capacitance part of the instrument, constant-phase element (CPE), and the completed equation was applied to obtain the virus capacitances from their impedance spectra. An applied AC bias of 10 mV was used to stay below the Johnson noise at room temperature of 26 mV, thereby minimizing electrical perturbations to the materials in the system. The impedance measurement was integrated over 10 s for each frequency below 100 Hz, in an attempt to average out low frequency noise sources from building vibrations and AC power lines. The impedance measurement was integrated for 1 s at each frequency at and above 100 Hz.

Results and Discussion

After a noncontact mode image was collected to find isolated virus particles on Au substrates (Figure 2), the AFM tip was moved to the center of a virus particle precisely through the closed-loop scanner. A constant tip force of 100 nN was applied to each virus to maintain the sufficient and consistent contact between AFM tip and virus. Before and after carrying out capacitance measurements, the system conductance was checked by measuring impedances of bare Au plates.[13] We first analyzed the dielectric properties of polymer nanoparticles as a function of AC frequency to study a circuit model of our system (Figure 3). Capacitances of PS and PMMA particles in the diameter of 100 nm were also compared at 90% of humidity as controls, and the capacitance of PMMA appeared higher than the PS capacitance, as shown in Figure 4a, which is consistent with the order of their dielectric constants, 3.12 and 2.6, respectively.[16]

Figure 4b shows capacitances of five types of viruses: AV5, HSV1, SV40, MVA, and CPMV. Their impedance signals were averaged 1−10 s for each AC frequency at 10 mV of AC bias. For each type of virus, 50 different particles were measured and collected capacitance spectra were averaged with error bars and normalized by the size of each virus, as shown in Figure 4b. In this figure, SV40 showed the highest capacitance while AV5 had the lowest. This plot indicates that those viruses could be clearly distinguished by measuring their capacitance spectra. It should be noted that there was no change in capacitance of the viruses regardless of the tip forces within the range of 50−500 nN (Figure 4c). We were aware that the water condensation between AFM tip and virus could affect our capacitance measurements since the previous dielectric study of B-normal white blood cells showed that the dielectric permittivity of water was comparable to the ones for nuclear envelope, nucleoplasm, and cytoplasm of the human cells.[17] To examine the influence of the water condensation between the tip and virus, the capacitance of the virus was measured at humidity levels between 10 and 90%, as shown in Figure 4d. In this figure, there was no change in the virus capacitance regardless of the degree of humidity. This outcome indicates that the water condensation had little effect on virus capacitance measurements. We would also like to note that the water bridge contributes less to the overall capacitance measurement in the higher frequency range between 10^2 and 10^4 Hz. The influence of solvents surrounding the sample to the capacitance value is considerable at the lower AC frequency due to the ionic motions in the surrounding media. In all measured capacitance spectra, the noise caused by the ionic motions was significantly reduced above 10^2 Hz. Thus, by monitoring the virus capacitance in the higher frequency range where the ionic motion was reduced, the effect of the water condensation could be minimized in the capacitance measurement of viruses, as shown in Figure 4. This observation supports the validity of virus capacitance data measured in the range of 10^2−10^4 Hz. In this range, the signal noise was small enough not to influence the capacitance of viruses, which made the AC-SPM capacitance reliable as characteristic markers for the virus diagnosis.

Viruses can be modeled as spheres consisting of conductive media surrounded by isolating shells. In the frame of this simplified model, envelopes and capsids of viruses behave as insulating layers (Figure 1), and the polarization on those layers significantly influences overall viral capacitance as a function of AC frequency.[18] At low frequencies, the envelopes and the capsids offer significant barriers to current flow and the whole virus can be treated as an isolating particle. Herein, changes in the capacitance are only related to the size of the particle. At intermediate frequencies, the polarization of envelopes and capsids decreases and the dielectric properties of these layers govern the capacitance of viruses. At high frequencies, the envelopes and the capsids are minimally polarized and the capacitance measurements provide information about the viral

(16) Maliakal, A.; Katz, H.; Cotts, P. M.; Subramoney, S.; Mirau, P. *J. Am. Chem. Soc.* **2005**, *127*, 14655−14662.
(17) Polevaya, Y.; Ermolina, I.; Schlesinger, M.; Ginzburg, B. Z.; Feldman, Y. *Biochim. Biophys. Acta* **1999**, *1419*, 257−271.
(18) Cheung, K.; Gawad, S.; Renaud, P. *Cytometry* **2005**, *65A*, 124−132.

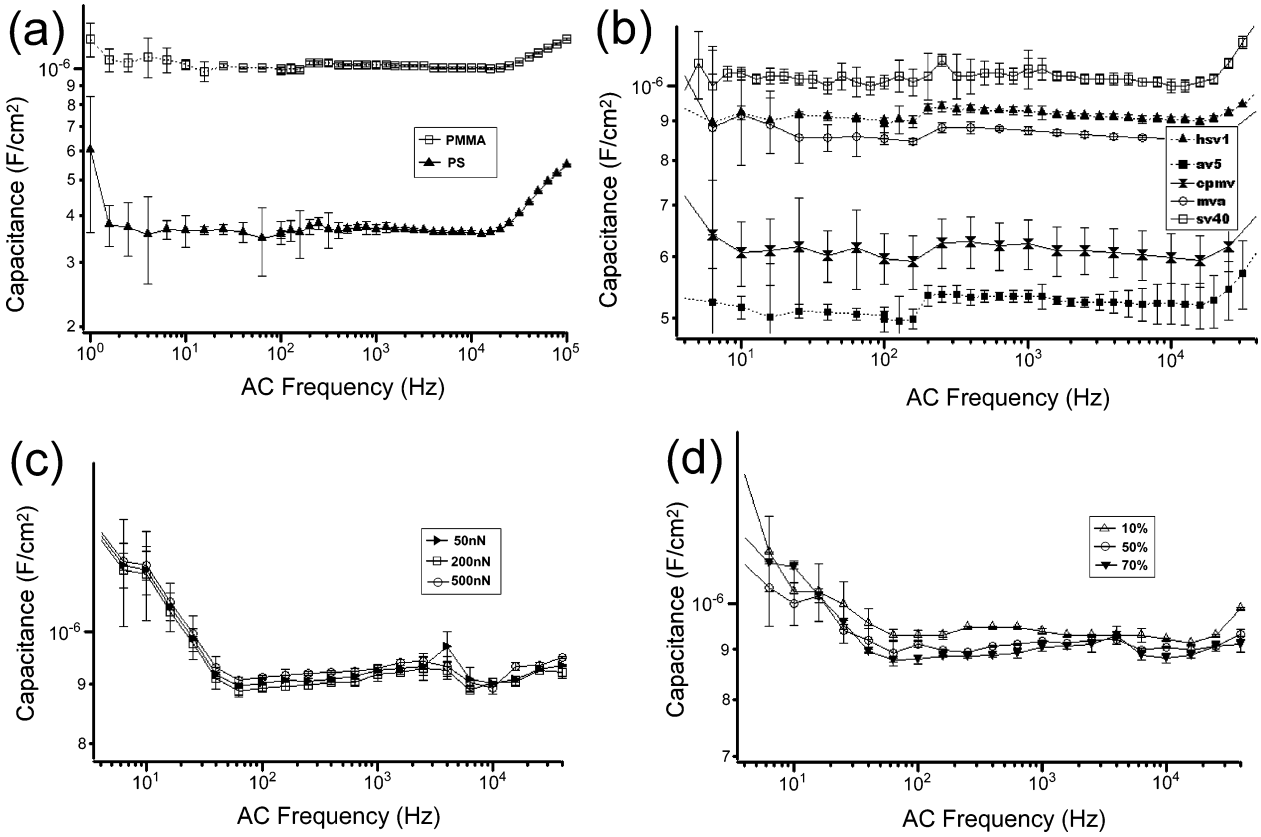

Figure 4. Capacitance spectra of (a) PMMA and PS nanoparticles, (b) AV5, CPMV, MVA, SV40, and HSV, (c) HSV1 with the tip forces, 50 nN, 200 nN, 500 nN, and (d) HSV1 at humidity levels 10, 50, and 70%.

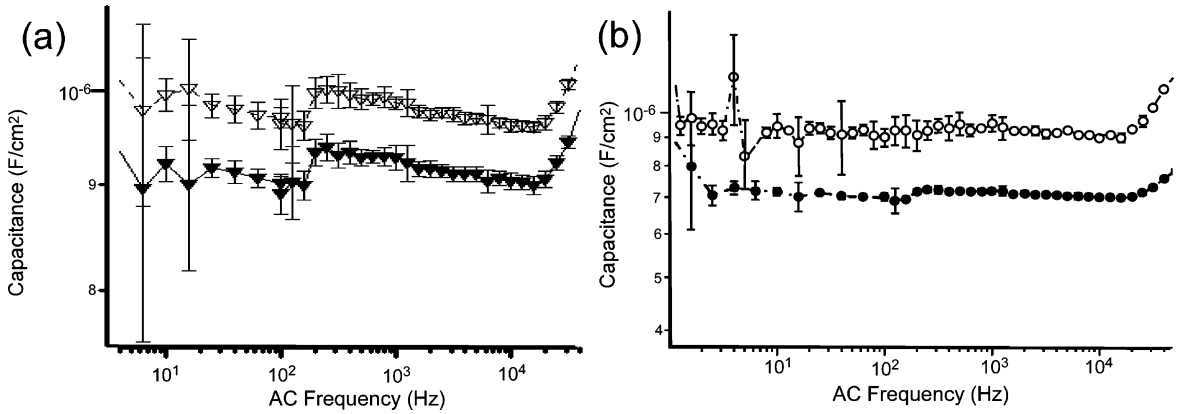

Figure 5. Capacitance spectra of (a) HSV1 (▼) and mutated HSV1 adding GFP in capsid (▽) and (b) HSV2 (○) and envelope-extracted HSV2 (●).

core (Figure 1). On the basis of this model, we hypothesize that the origin of the capacitance difference among viruses in our measurements arises from differences between the dielectric properties of characteristic glycoproteins in their envelopes and capsid proteins in their capsids since we measured viral capacitances in the intermediate frequency range. Unfortunately, exact dielectric constants and distributions of the specific proteins in these viruses are not well characterized, and therefore overall dielectric constants of those viruses cannot be directly compared with our observation in Figure 4b to confirm our hypothesis. However, the dielectric variations of viruses could be inferred from the differences of capacitance values between wild-type and modified viruses; glycoproteins can be modified by mutation or capsid proteins can be removed chemically. Here we designed two separate control experiments to probe whether capacitance measurements are sensitive to proteins in the capsid and the envelope. First, HSV1 was mutated to add green fluorescence proteins (GFP) in their capsid and compared with the wild type of HSV1. As shown in Figure 5a, GFP-mutated HSV1 has a higher capacitance as compared to the wild-type HSV1. The GFP, whose isoelectric point is 5.5, charges negatively in neutral pH and physiological pH buffers,[19] and this dielectric difference in the capsid shifts the capacitance of GFP-mutated HSV1 higher than the capacitance of wild-type HSV1. For the second control experiment to probe the effect of glycoproteins in the envelopes on virus capacitances, we extracted envelopes of HSV2 chemically using the freon extraction method and compared capacitances between the

(19) Jena, S. S.; Bloomfield, V. A. *Macromolecules* **2005**, *38*, 10551−10556.

envelope-extracted HSV2 and the wild-type HSV2. As the envelope of HSV2 was removed, the capacitance decreased, as shown in Figure 5b. Since viruses of the same viral strain have the same dimension and inner content, the observed changes in capacitance are related to the dielectric properties of the viral envelopes and capsids. Thus, these results indicate that proteins in the envelope and the capsids contribute significantly to the overall dielectric constant of HSV at the intermediate frequencies. Moreover, it indicates that our capacitance measurements were performed at the proper frequency range, thus validating the proposed methodology for detecting viruses via their characteristic envelope/capsid compositions.

It should be noted that the previous study on dielectric properties for various populations of white blood cells also supports our hypothesis about the origin of the characteristic capacitance responses for different viruses.[17] In this work, dielectric permittivity, capacitance, and conductivity of the human cells were broken down into each component such as membrane (first shell), cytoplasm, nuclear envelope (second shell), and nucleoplasm with the double-shell dielectric model. Although this work studied dielectric permittivity, capacitance, and conductivity of the human cells, the viral structure also consists of two shells, envelope and capsid, and their outcome was consistent with our viral results in capacitance values. However, even more significant is that conductivities and capacitances for two shells of those cells, membranes and nuclear envelopes, were highly characteristic of the types of cells. Since we also found in the case of viruses that proteins in two viral shells, envelopes and capsids, had significant effect on the overall capacitance of viruses as shown in Figure 5, the offsets of capacitance values in different viral systems in Figure 4b also likely appeared due to the characteristic capacitance differences in envelopes and capsids among viruses.

Conclusions

AC capacitance scanning probe microscopy showed that five viruses, AV5, CPMV, MVA, SV40, and HSV1, possessed distinguishable and characteristic capacitances. A mutation on the capsid in HSV1 with GFP increased capacitance from 9×10^{-6} to 1×10^{-5} F/cm^2 at 10^4 Hz. HSV2 decreased capacitance when its envelope and glycoproteins were chemically extracted. These control experiments indicate that dielectric properties of capsid proteins and glycoproteins significantly influence the observed overall capacitances of viruses. Because those capsid proteins and glycoproteins are characteristic of the viral type, this AC-SPM technique could be applied to detect and identify viruses at the single viron level using their distinct capacitance spectra as fingerprints without labeling.

Acknowledgment. This work was supported by the U.S. Department of Energy (DE-FG-02-01ER45935) and the National Institutes of Health (2-S06-GM60654). Hunter College infrastructure is supported by the National Institutes of Health, the RCMI program (G12-RR-03037). H.M. thanks Prof. John Johnson for providing CMPV samples and Drs. Phillip Krause and Andrea Bertke for the donation of viruses. H.M. also appreciates the very useful discussions with Drs. Igor Kuskovsky, Shigeo Yoshii, and Roberto de la Rica. R.I.M. thanks Dr. Keith Jones for assistance with AFM modifications.

JA075244Z